

Numerical Simulation of Neutral Dynamics in Stationary Short - Gap Discharge in Air

M. Lemerini¹, B. Bouhafs¹, B. Benyoucef¹ and A. Belaïdi²

¹ Institut des Sciences Exactes, Université Aboubekr Belkaïd
BP 119, Tlemcen 13000, Algérie

² Electrical Engineering Department, E.N.S.E.T, Oran 31000, Algérie

(Accepté le 27.10.99)

Résumé - Nous simulons numériquement les effets thermiques produits dans l'air (760 Torr) par une décharge électrique stationnaire de faible courant. Nous proposons une fonction mathématique qui simule l'injection de l'énergie dans le gaz. La décharge simulée est de type pointe positive plan négatif, de distance inter électrodes égale à 6 mm et possédant la symétrie de révolution autour de l'axe de la décharge. L'évolution spatio-temporelle des neutres est analysée sur la base des équations classiques de la dynamique des fluides, c'est-à-dire équations de continuité, de la quantité de mouvement et de l'énergie, dans un espace à deux dimensions (géométrie de révolution cylindrique). Nous avons adopté pour la résolution du système, la procédure dite F.C.T. (Flux Corrected Transport), dont le principe réside dans l'application d'une diffusion correctrice au profil issu d'un schéma dispersif, en localisant cette diffusion uniquement dans les régions où des oscillations ont tendance à se produire.

Abstract - The numerical simulation of the variation of the neutral molecule density induced by the strong correlation between the dynamics of the electron gas and that of the neutral gas is studied in a 2-D numerical modelisation. The energy injection is simulated by a mathematical function that represents the spatial dependence of the discharge density. The simulated discharge is a positive point to plane discharge in a gap = 6 mm, in air at atmospheric pressure (760 Torr), with cylindrical symmetry. The hydrodynamic set of equations, i.e. equations of transport for mass, momentum and energy, is solved by the flux corrected transport (F.C.T.) method, in employing the procedure of time splitting for the two space variables. The space and time distributions of the fundamental hydrodynamic quantities, density and temperature of the neutral gas are obtained.

Mots clés: Décharge dans les gaz - Transfert d'énergie - Plasma froid - Phénomène de transport.

1. INTRODUCTION

During the inception and development of the plasma in a point to plane gas discharge, a spatio-temporel evolution of the temperature of the neutral gas occurs as a result of plasma-neutral molecules energy interaction. The temperature gradient causes a phenomenon of diffusion and convection as a result of the accompanied strong heterogeneity in the neutral gas density and pressure. The fundamental role of neutral heating in the inception of gas breakdown has been shown by theoretical studies [1-3], as well as by experimental studies [4, 5]. The behaviour of a point to plane discharge has been optically and electrically analysed for a centimetric gaps in air at atmospheric pressure. [6]

This study has shown that, if a steady high voltage is applied to the point through a high value resistance, and induced discharge appears above a threshold value V_s , the discharge is not steady but composed of a succession of individual discharges. For a potential greater than V_s , some of these individual discharges develop completely into transient arcs [7]. On the thermodynamically point of view, for the neutral gas, this corresponds to an energy injection which increases its temperature and gives rise to convective movements.

In this paper, we study the thermodynamics of the neutral gas subjected to energy injection as the result of electric discharge in the considered medium. This approach to the problem allows to consider the discharge only on its energetic aspect. The discharge plays the role of an injection in the gas. To define the profile of this energy injection, we propose a mathematical function that represents the spatial dependence of the discharge density. The spatio-temporal evolution of the neutral gas particles is studied on the basis of hydrodynamic set of equations, i.e. equations of transport for mass, momentum and energy. The simulated discharge is a positive point to plane discharge [6]. The simulation of the discharge in space is two-dimensional (i.e. r, z) with cylindrical symmetry. The hydrodynamic set of equations is solved by the flux corrected transport [8, 9] (F.C.T.) method using the procedure of time splitting for the two space variables. The space and time distributions of the fundamental hydrodynamic quantities, density, transport velocity and temperature of the neutral gas are obtained.

2. MODELING OF THE NEUTRAL DYNAMICS

2.1 Basic equations

The formalism is that of hydrodynamics with the hypothesis of a slightly ionised gas. We assume that the energy injection is weak enough to avoid molecules dissociation. Air is considered as a monomolecular gas with well known properties of conduction and viscosity. The point to plane discharge is supposed with revolution symmetry along the axis of the discharge, and thus the 2-D model used for its simulation is a bidimensional model in r and z . The continuity equation for neutral particles is :

$$\frac{\partial N}{\partial t} + \nabla \cdot (N \mathbf{V}) = 0 \quad (1)$$

where N is the density of the neutral gas, and \mathbf{V} their total velocity.

In this model we neglected the momentum transfers from charged particles to neutral molecules. In fact, in slightly ionised gases discharges, it can be considered that convective movements in the gas are mainly due to temperature and pressure gradient, more active than the direct momentum transfers.

So, the equation for velocity of the neutral particles is :

$$\frac{\partial \mathbf{V}}{\partial t} + \nabla \cdot (\mathbf{V} \mathbf{V}) = -\frac{1}{M N} \nabla P - \frac{1}{M N} \nabla \bar{\bar{\Gamma}} \quad (2)$$

where M is the mass of the gas molecules, P the pressure of the neutral molecules and $\bar{\bar{\Gamma}}$ the viscosity tensor.

In cylindrical coordinates, the components of the viscosity tensor can be written as :

$$\text{component following } r\text{-axis: } \left[\nabla \bar{\bar{\Gamma}} \right]_r = \frac{1}{r} \frac{\partial}{\partial r} (r \tau_{rr}) - \frac{\tau_{\theta\theta}}{r} + \frac{\partial \tau_{rz}}{\partial z} \quad (3)$$

$$\text{component following } z\text{-axis: } \left[\nabla \bar{\bar{\Gamma}} \right]_z = \frac{1}{r} \frac{\partial}{\partial r} (r \tau_{rz}) + \frac{\partial \tau_{zz}}{\partial z} \quad (4)$$

where $\tau_{rr}, \tau_{zz}, \tau_{rz}, \tau_{\theta\theta}$ are the components of the viscosity tensor.

The energy injected in the resistive neutral medium by time unity is transformed in different forms (rotational and vibrational energy, electronic excitation, thermal energy,

ionisation). Taking into account our time schedule analysis, it can be assume that only the translation, the rotational and an important part of the electron excitation energy immediately relax in thermal energy. So, the energy equation for neutral molecules can be written as :

$$\frac{\partial W}{\partial t} + \nabla \cdot (W \cdot V) = \Phi(r, z, t) + \lambda \nabla^2 T - \nabla \cdot (P \bar{I} + \bar{\Gamma}) V \quad (5)$$

where \bar{I} is a unit matrix, W the total energy and $\Phi(r, z, t)$ represents the part of energy injected by the discharge and transformed in thermal energy. The choice of the function $\Phi(r, z, t)$ allows to adjust the spatial localisation of the energy injection. The results presented afterwards correspond to a major injection of energy at the vicinity of the point, as shown by the experimental results obtained by interferometry. [6]

To close the system composed by eq. (1), (2) and (5), we added the equation of state (perfect gas):

$$P = N k T \quad (6)$$

where k is the Boltzmann constant and T the gas temperature.

2.2 Numerical scheme

The transport equations for density, momentum and energy can be written on the generalised form:

$$\frac{\partial}{\partial t}(\rho \phi) + \nabla \cdot (\rho \phi \cdot V - v_\phi \nabla \phi) = S_\phi \quad (7)$$

where ρ is the volumetric mass, ϕ the transported physical property, v_ϕ the diffusion coefficient and S_ϕ the source term. We used the method of finite volumes based on the macroscopic balances.

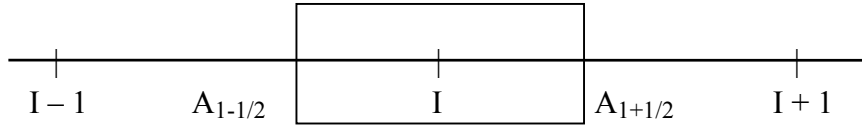
This method provides a greater generality than other methods, like finite elements or finite differences, specially for the solution on intricate outflows near the walls. [10]

For this purpose, the analysed area is sliced in a set of cells (control volumes), non overlapping each others, and surrounding each node of the discretisation network. The finite volume method takes into account the preservation principle of the physical property ϕ in an elementary cell. The preservation of the property is available for any set of cells, and thus in the whole domain, whatever the node number.

The time splitting scheme allows to replace the integration of multidimensional equation, by successive monodimensional integrations in r and z directions. Along a direction x (may it be r or z), eq. (7) can be integrated as :

$$\tau_i \left[(\rho \phi)_i^n - (\rho \phi)_i^0 \right] + A_{i+\frac{1}{2}} \int_t^{t+\delta t} \left(\rho \phi v_x - \gamma_\phi \frac{\partial \phi}{\partial x} \right)_{i+\frac{1}{2}} dt + A_{i-\frac{1}{2}} \int_t^{t+\delta t} \left(\rho \phi v_x - \gamma_\phi \frac{\partial \phi}{\partial x} \right)_{i-\frac{1}{2}} dt = S_i^0 \tau_i \delta t \quad (8)$$

where τ_i is the value of control's volume, S_i the value of surface and $A_{i\pm\frac{1}{2}}$ the values at $i \pm \frac{1}{2}$ of the surface between control volumes.



For the explicit centred scheme, the relation (8) can be written as:

$$\begin{aligned} \tau_i (\rho \phi)_i^n = & \tau_i (\rho \phi)_i^0 + A_{i-\frac{1}{2}} \delta t \left\{ \frac{1}{2} \left[(\rho \phi v_x)_i^0 + (\rho \phi v_x)_{i-1}^0 \right] - v_{\phi_{i-\frac{1}{2}}} \left(\frac{\phi_i^0 - \phi_{i-1}^0}{x_i - x_{i-1}} \right) \right\} \\ & - A_{i+\frac{1}{2}} \delta t \left\{ \frac{1}{2} \left[(\rho \phi v_x)_{i+1}^0 + (\rho \phi v_x)_i^0 \right] - v_{\phi_{i+\frac{1}{2}}} \left(\frac{\phi_{i+1}^0 - \phi_i^0}{x_{i+1} - x_i} \right) \right\} + S_i^0 \tau_i \delta t \quad (9) \end{aligned}$$

To correct this disperse effects of the scheme, the flux corrected technique developed by Boris and Book [9] are used.

2.3 Boundary conditions

The study domain is defined by figure 1. The limit velocity of the molecules on the surface is assumed equal to zero. As it is necessary to take into account the local heating effects, the temperature of the surface is assumed equal to the averaged temperature of the surrounding gas, and the temperature of the electrode body is assumed invariable and equal to the ambient temperature. On the axis :

$$\frac{\partial N}{\partial r}(0, z, t) = \frac{\partial T}{\partial r}(0, z, t) = \frac{\partial V}{\partial r}(0, z, t) = V(0, z, t) = 0 \quad (10)$$

The initial conditions are : gas density $N(r, z, 0) = 2.5 \cdot 10^{19} \text{ cm}^{-3}$ for $T(r, z, 0) = 293 \text{ K}$, the pressure $P(r, z, 0) = 760 \text{ Torr}$ and $U(r, z, 0) = 0$ in a quiescent surrounding gas.

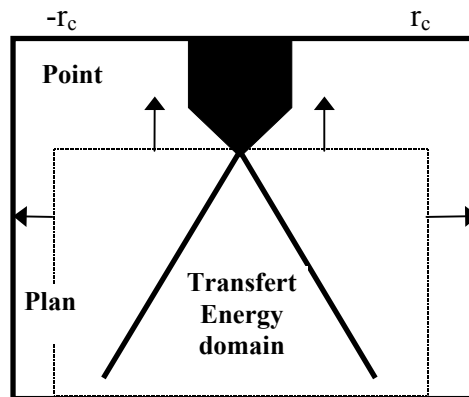


Fig. 1: Domain study

3. RESULTS AND DISCUSSION

The profile of the injection energy is defined by :

$$\Phi(r, z) = C J_0 \left(2.405 \frac{r}{r_c} \right) \cdot \sin \left(\frac{\pi}{2} \frac{(d - z)}{d} \right) \quad (11)$$

where r is the radius, $r_c = 0.15$ mm is the extension radius of the energy injected (with regard to the axis), $d = 6$ mm the distance point to plane (with regard to the plane), J_0 is the zero order Bessel function and C a parameter which is adjusted to represent the energy injected by volume unity. The “ Bessel ” radial dependence and the sinusoidal axial dependence are essentially a consequence of inhomogeneous ionic and electronic densities observed by Vennin et al. [6].

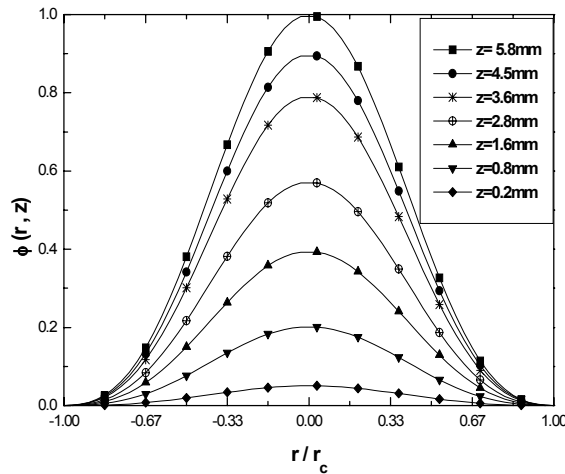


Fig. 2: Normalised profiles of terms of energy transfer

The spatial evolution of the main values of the neutral gas (temperature and density) are shown in figures 3, 4, 5 and 6, where we show the interaction between the neutral and the charged particles.

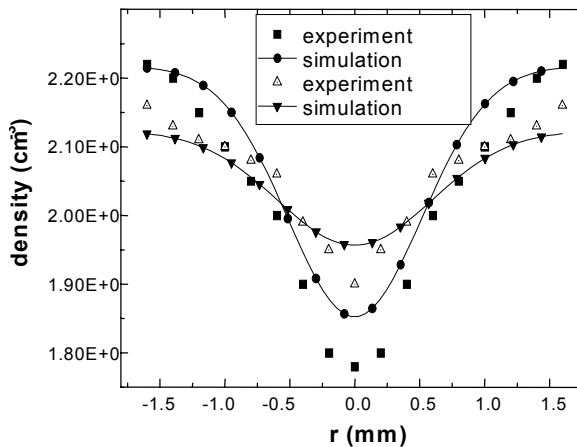


Fig. 3: Comparison of the radial neutral density profile from experiment and numerical model at two positions ($z = 4.5$ mm and $z = 2.5$ mm, $z = 6$ mm represent the anode and $z = 0$ mm represent the cathode)

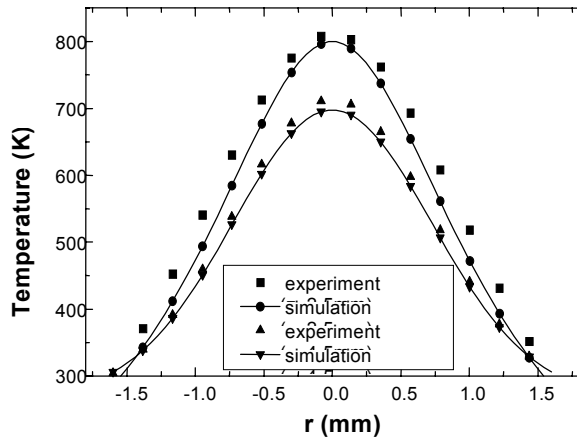


Fig. 4: Comparison of the radial neutral temperature profile from experiment and numerical model at two positions ($z = 4.5$ mm and $z = 2.5$ mm, $z = 6$ mm represent the anode and $z = 0$ mm represent the cathode)

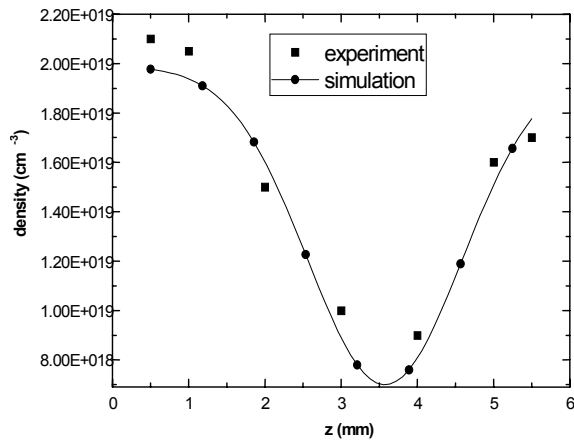


Fig. 5: Comparison between experiment and numerical profile of the neutral density along the discharge axis

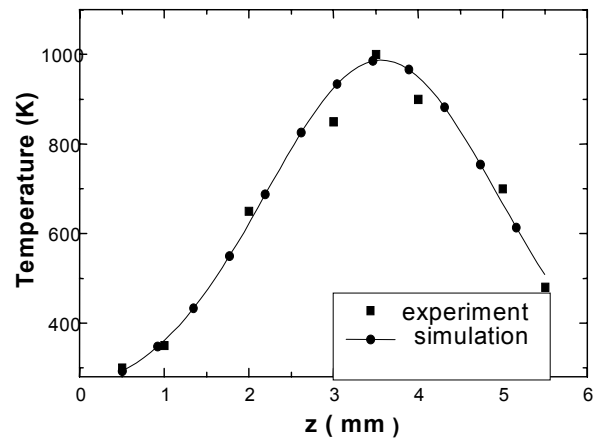


Fig. 6: Comparison between experiment and numerical profile of the neutral temperature along the discharge axis

The examination of the first set of curves (Fig. 6) shows the evolution of the neutral gas temperature at different points along the axis of the discharge. We can see heating process is different from one point to another, owing to spatial distribution of injected energy. Until $t = 2 \mu\text{s}$, the energy transfer from ionised gaseous to neutral gas is greater than dissipation by thermal conductivity. So the temperature increases rapidly in places where the injection is maximum.

The convective movements which depended essentially on pressure gradient react immediately to this increasing of the temperature, so more exactly to ∇T which $N \approx \text{constant}$, and the energy is dissipated rapidly. In so doing this creasing is followed by a stabilisation from $5 \mu\text{s}$. It can be noted that the maximum of the temperature (900 K) and the minimum of the density ($1.05 \cdot 10^{19} \text{ cm}^{-3}$), are localised at a distance equal to $(d/3)$ from the plane, these numerical results confirm the experimental results (6).

Figure 7 gives the evolution of the rate of neutral de population $(N_0 - N)/N_0$, N_0 being the initial density. Clearly we observed on these set of curves, that the depopulation depends on the local variation of temperature. So the depopulation rises from the point ($z = 1 \text{ mm}$) and during the time moved to the plane. This is a consequence of axial propagation of thermal wave. The maximum value reached by the depopulation rate at $t = 5 \mu\text{s}$ (stabilisation phase) is equal to 70 % at $z = 3 \text{ mm}$, and the minimum is equal to 50 % at $z = 1 \text{ mm}$. This shows that the variation is governed by spatial current density (or injected energy) distribution.

Figure 8 shows the effects of axial pressure gradients. This wave propagates in a medium set in movement due to direct momentum transfer. We can see that the acoustic wave's velocity is equal to 340 m/s. We can see that the heating process is more important in the axis than elsewhere ($r > 0$). It's the consequence of the important energy transfer in this region.

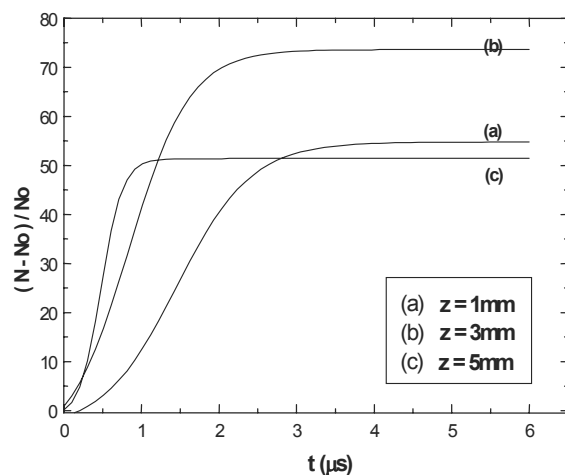


Fig.7: Temporal evolution of neutral density for three positions along the discharge axis - (a): near the cathode, (b): at the middle of the discharge, (c): near the anode

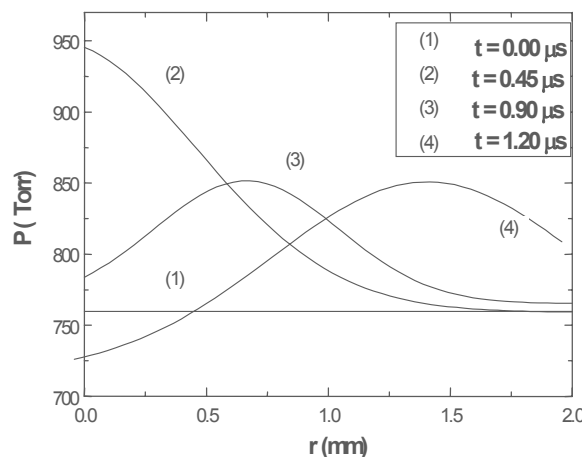


Fig. 8: Radial profile of neutral pressure from different instants ($0 \mu\text{s}$, $0.45 \mu\text{s}$, $0.90 \mu\text{s}$ and $1.20 \mu\text{s}$)

4. CONCLUSION

In conclusion it can be said that the present numerical calculations have demonstrated that the mathematical formalism suggested is suitable for the modelling of neutral thermal imprint. This study shows also that the stabilisation of the neutral gas is mainly function of the energy injection distribution, and the neutral gas is not considered like an infinite energy absorber.

So, as soon as a current goes through the neutral gas, obviously a joule heating effect increases locally the temperature. It results a neutral movement which has for aim to make uniform the pressure in the system.

REFERENCES

- [1] G.L. Rogoff, Phys. Fluids 15, 1931 - 1940, (1972).
- [2] E. Marode, F. Bastien and M. Bakker, J. Applied Physics, 50, 140 - 146, (1979).
- [3] J. Dupuy and A. Gibert, J. Phys. D: Appl. Phys. 15, 655, (1982).
- [4] I.D. Chalmers, I. Gallimberti, A. Gibert, O. Farish, Proc. R. Soc. A 412 285, (1987).
- [5] M. Goldmann and A. Goldmann, '*Corona discharge in gaseous electronics*', ed. By J.N.Hirsh, H.J. Oskam, Acad. Press 1978..
- [6] C. Vennin, A. Chakari, P. Bayle, X int. Conf. On gas discharges, Swansea (G.B). 1992.
- [7] R.S. Sigmond, '*Coronas discharges in electrical breakdown of gases*', ed. J.M. Meek and J.D. Craggs, Wiley New-York (1978).
- [8] J.P. Boris, D.L. Book, '*Flux corrected transport. I.SHASTA, a transport algorithm that works*', J. of Computational Physics, 11, 38 - 69 (1973).
- [9] D.L. Book, '*Finite difference technique for vectored fluid dynamic calculation*', ed. Springer-verlag, 1981.
- [10] S.V. Patankar, '*Numerical heat transfer and fluid flow*', Mac Graw-Hill, 1980.